

The redshift distribution of gamma-ray bursts revisited

P. Natarajan^{1,2}, B. A. Ianna^{2,3}, J. Hjorth⁴, E. Ramirez-Ruiz⁵, N. Tanvir⁶ & R. Wijers⁷

¹ Astronomy Department, Yale University, P.O. Box 208101, New Haven, CT 06520-8101, USA

² Department of Physics, Yale University, P.O. Box 208101, New Haven, CT 06520-8101, USA

³ Department of Physics, Univ. of California at Berkeley, 366 Le Conte Hall, Berkeley, CA 94720-7300, USA

⁴ Niels Bohr Institute, University of Copenhagen, DK-2100 Copenhagen, DENMARK

⁵ Institute for Advanced Study, Princeton, NJ, USA

⁶ Centre for Astrophysics Research, University of Hertfordshire, College Lane, Hatfield AL10 9AB, UK

⁷ Astronomical Institute, Faculty of Science, University of Amsterdam, Kruislaan 403, 1098 SJ Amsterdam, The Netherlands

30 November 2018

ABSTRACT

In this letter, we calculate the redshift distribution of gamma-ray bursts assuming that they trace (i) the globally averaged star formation rate or (ii) the average metallicity in the Universe. While at redshifts 5 and below, both the star formation rate and metallicity are observationally determined modulo some uncertainties, at higher redshifts there are few constraints. We extrapolate the star formation rate and metallicity to higher redshifts and explore models that are broadly consistent with bounds on the optical depth from WMAP results. In addition, we also include parametric descriptions of the luminosity function, and the typical spectrum for GRBs. With these essential ingredients included in the modeling, we find that a substantial fraction 75% of GRBs are expected to originate at redshifts below 4, in variance with some previous estimates. Conversely, if we assume as expected for the collapsar model that gamma-ray bursts favour a low metallicity environment and therefore, relate the GRB rate to a simple model of the average metallicity as a function of redshift, we find that a higher fraction of bursts, about 40% originate from $z > 4$. We conclude with the implications of SWIFT GRB detections.

Key words:

1 INTRODUCTION

The demonstration that long-duration gamma-ray bursts (GRBs) are related to core-collapse supernovae (Galama et al. 1998; Stanek et al. 2003; Hjorth et al. 2003; Malesani et al. 2004), likely leading to the formation of black holes in ‘collapsars’ (MacFadyen & Woosley 1999) suggests, that GRBs trace the deaths (and hence births) of short-lived massive stars. Moreover, as GRBs can be detected to very high redshifts (Lamb & Reichart 2000), unhindered by intervening dust (the current record is $z = 4.50$ (Andersen et al. 2000)) they hold the promise of being useful tracers of star formation in the Universe (Wijers et al. 1998; Totani 1997; Blain et al. 1999; Blain & Natarajan 2000; Ramirez-Ruiz, Trentham & Blain 2002; Bromm & Loeb 2002; Gou et al. 2004). This ansatz, that GRBs are likely to effectively trace the observed star formation rate (SFR), has been used to predict the redshift distribution of GRBs, despite our lack of knowledge of SFRs at $z > 6$. Observational estimates of the SFR even at modest redshifts have been plagued by uncertainties arising due to correction for dust extinction. Therefore, SFR’s need to be extrapolated to higher redshifts. The only current constraint that is useful is the

WMAP (Wilkinson Microwave Anisotropy Probe) estimate of the optical depth and the redshift of re-ionization (Kogut et al. 2003), both of which suggest the existence of ionizing sources out to very high redshifts. The extrapolations of the SFR explored here would provide the requisite number of ionizing photons as demonstrated by Somerville & Livio (2003).

The discovery of several $z \sim 6$ quasars in the SDSS (Sloan Digital Sky Survey) whose spectra are consistent with showing zero flux below Lyman- α (a Gunn-Peterson’ trough) indicates that the IGM (Inter-Galactic Medium) had a significant neutral fraction at $z > 6$ (Fan et al. 2001; Becker et al. 2001). The ionization history of the Universe has also been constrained via observations of the cosmic microwave background (CMB). The first-year results from the WMAP satellite constrain the optical depth to Thomson scattering to be $\tau = 0.17 \pm 0.04$, implying a re-ionization redshift $z_{\text{reion}} = 17 \pm 5$ (Kogut et al. 2003). Our extrapolation of the SFR to higher redshifts is in consonance with these observations.

In this work, we explore a fully self-consistent approach to predict the expected redshift distribution of GRBs at

$z > 3$. In section 2, the observed redshift distribution of GRBs is presented. A clutch of star formation models are studied here, which are then extrapolated to higher redshifts. In section 3, we also investigate the proposition that GRB progenitors might be preferentially metal-poor as expected in the collapsar model and as suggested by the observations of Fynbo et al. (2003) & Vreeswijk et al. (2004). A model where the GRB rate, is inversely correlated to the mean metallicity in the Universe is explored. GRBs are then modeled with a typical spectral shape and a luminosity function, the details of which are presented in section 4. We conclude with a synopsis and discussion of our results in the context of GRB detections by the SWIFT satellite in section 5.

2 GRBS: THEIR OBSERVED REDSHIFT DISTRIBUTION AND THE STAR FORMATION RATE

Despite the ability of spacecraft equipped with GRB detectors to detect GRBs to high redshift (Gorosabel et al. 2004), no very high- z GRB has yet been detected at say, $z > 5$. It is important to note that selection effects are difficult to quantify so the observed distribution may not be the same as the true distribution. Two of the primary causes of selection effects are the lack of knowledge of the intrinsic luminosity function of GRBs and the details of the central engine that drives the bursts both of which impact the redshift distribution of bursts.

The recent launch of Swift promises to detect GRBs en masse (Gehrels et al. 2004). It is interesting to note that $z_{\text{median}} = 1.1$ for non-SWIFT bursts, and $z_{\text{median}} = 2.9$ for SWIFT bursts, bolstering hopes that SWIFT may indeed push detection of GRBs more efficiently to higher redshifts. While the calibration of the detection efficiency for SWIFT will be best determined over the next couple of years of operation, for the purposes of this paper we use the detection efficiency model curve for SWIFT adopted by several other authors (Gou et al. 2004; Gorosabel et al. 2004 (Fig. 3); Porciani & Madau 2001). The detection efficiency curve as a function of redshift that we adopt is overplotted in Fig. 2 (thin solid line).

To what extent do GRBs trace star formation? It has been argued that individual GRBs may trace galaxies or regions of galaxies with high specific star formation (Christensen et al. 2004; Courty et al. 2004) or low metallicity (Fynbo et al. 2003; MacFadyen & Woosley 1999; Ramirez-Ruiz et al. 2002). However, this does not preclude the possibility that GRBs trace the star-formation rate of the Universe in a globally averaged sense. Indeed, the luminosity function (LF) of $z > 2$ GRB host galaxies, assuming GRBs trace UV light, and the LF of Lyman-break galaxies are consistent (Jakobsson et al. 2005). We start with the premise that the GRB rate¹ traces the global SFR of the Universe, $R_{\text{GRB}}(z) / R_{\text{SF}}(z)$, where $R_{\text{SF}}(z)$ is the comoving rate density of star formation.

The expected evolution of the globally averaged cosmic

SFR with redshift has been studied by many authors, following the first successful attempt by Madau et al. (1996), who based their estimates on the observed (rest-frame) UV luminosity density of galaxy populations. Using various observational techniques, the cosmic SFR can now be traced to $z \sim 5$, although there is no clear consensus on the details of dust correction both at high and low redshifts (Dickinson et al. 2003; Steidel et al. 2004). In this paper, we explore several models that describe (all shown in Fig. 1) the global SFR per unit comoving volume. Wherever needed, values for cosmological parameters consistent with the WMAP results (Spergel et al. 2003) are assumed: matter density $\Omega_m = 0.3$, baryon density $\Omega_b = 0.044$, dark energy $\Omega_\Lambda = 0.70$, Hubble parameter $H_0 = 70 \text{ km/s/Mpc}$, fluctuation amplitude $\sigma_8 = 0.9$, and a scale-free primordial power spectrum $n_s = 1$.

The first model studied here (Model I hereafter) is similar to one considered previously by Porciani & Madau (2001) which they used in modeling the fraction of lensed GRBs (their model SF3). Our Model I (dotted curve in Fig. 1) provides a good fit to the sub-mm determinations of the luminosity density. Blain et al. (1999) have argued that the SFR at all redshifts may have been severely underestimated due to large amounts of dust extinction detected in SCUBA galaxies. In addition, we construct a high redshift extrapolation for a SF history (Model II, the solid curve in Fig. 1) that is required to fit the observational data at low redshifts and has sufficient star formation at high redshifts ($z > 10$) to match the WMAP constraints on the optical depth. We justify this extrapolation with a physical picture in mind using a semi-analytic model, the details of which are described in the following section. Models I and II predict very similar GRB rates although they appear to be divergent at $z > 7$. Finally, as GRBs themselves do not seem to be pointing to large amounts of dust in their host galaxies (Berger et al. 2003; Tanvir et al. 2004; Fynbo et al. 2003; Jakobsson et al. 2005; Vreeswijk et al. 2004), and while this might be a selection effect, we have also considered a model in which the bulk of the star formation is not obscured by dust at $z > 5$ but occurs in a population of numerous very faint galaxies that each may have moderate amounts of dust (our Model III). We have used the lower limit on the SFR from observations of Lyman-break galaxies at $z \sim 5$ to constrain our Model III (dashed curve in Fig. 1).

2.1 Constructing Model II: a semi-analytic model for high redshift star formation

We calculate the global SFR density from $z \sim 30$ to $z \sim 3$ using a simple model that combines the rate of dark matter halo growth with a prescription for cooling and star formation and match this rate to observational constraints on the SFR obtained at $3 < z < 6$ and at lower redshifts (similar to previous work by Somerville & Livio 2003). Prompted by the WMAP estimate of the optical depth at re-ionization, which points to the existence of a significant number of ionizing sources at high redshift (assumed to be stars), we construct a SF history with vigorous activity at the earliest epochs. This is done in the context of the standard structure formation scenario within the cold dark matter paradigm, where halos build-up hierarchically and galaxies form from the condensation of baryons in dark halos. A much more sophisticated version of this approach was pioneered (Kaumann et al.

¹ Throughout this paper GRB rate refers to the GRB occurrence rate and not the detected rate unless explicitly stated.

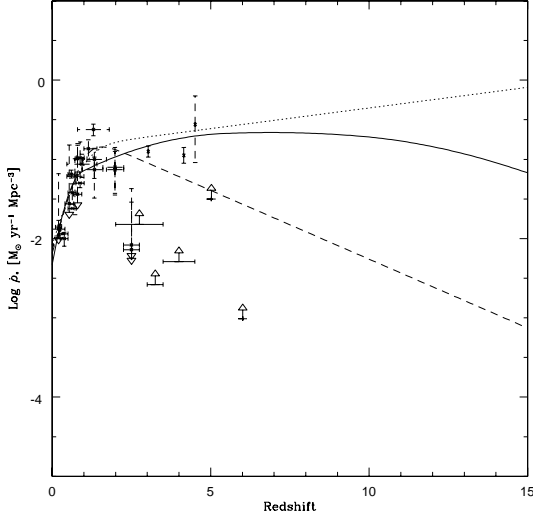


Figure 1. The three star formation models considered in this work Model I (dotted curve); Model II the constructed semi-analytic model (solid curve) and the conservative Model III (short dashed curve). The data points (with error bars) are collated from the literature of measured star formation rates from various authors, this particular compilation was taken from a paper by Dickinson et al. (2003) and references therein.

1993; Cole et al. 1994), developed and honed over the years by several groups.

With the abundance of dark matter halo masses $(M; z)$ determined using the Press-Schechter formalism, we then proceed to use a simple cooling criterion to determine the fraction of gas that is converted into stars modulo some efficiency factor² taken to be roughly 10% in these collapsed halos. Depending on the primary coolant, atomic or molecular, there is a critical mass threshold for a dark matter halo's gas content to cool, and form stars. The star formation rate can then be written as follows:

$$\dot{M}_* = \bar{\rho}_b \frac{df_m}{dt} (M > M_{\text{thres}}); \quad (1)$$

where f_m is the fraction of the total mass in collapsed halos with masses greater than M_{thres} , obtained from the halo mass function $dn(M; z) = dM$, $\bar{\rho}_b$ is the mean density of baryons and the efficiency of converting gas into stars is encapsulated in f_m . The threshold mass M_{thres} determines the dominant cooling route, it corresponds to halos with a virial temperature of about 10^4 K for atomic cooling, and $T \sim 100$ K for molecular cooling. Using standard cooling arguments and assuming a Salpeter IMF for the stars formed, the SF rate can be computed. The predicted SFR for this model (solid curve in Fig. 1) is then calibrated with observational estimates at 'low' redshift $3 < z < 6$. Using Somerville & Livio's estimates for the fraction of ionizing photons available per hydrogen atom given the SFR, we argue that these SFR models are consistent with the optical depth measured by WMAP (for further details see Section 4.2 of Somerville & Livio 2003).

² The requirement to match up with the measured value of the SF at $z = 0$ constrains the value of f_m to 10%.

2.2 GRB rate and metallicity: exploring a toy model

A larger proportion of the higher redshift GRB host galaxies are detected as Lyman-emitters (Kulkarni et al. 1998; Ahn 2000; Moller et al. 2002; Vreeswijk et al. 2004; Fynbo et al. 2003) compared to galaxies selected by the Lyman-break technique (Shapley et al. 2003) at similar redshifts. This led Fynbo et al. (2003) to suggest a preference for GRB progenitors to be metal-poor as predicted by the collapsar model. In the collapsar model, the presence of a strong stellar wind (a consequence of high metallicity) would hinder the production of a GRB, therefore metal-poor hosts would be favoured sites (MacFadyen & Woosley 1999; Izzard et al. 2004). Here, we explore a toy model wherein the GRB rate decreases with increasing metallicity. There are observational constraints on the mean metallicity of the Universe as a function of redshift (Pettini 2003), however, for our exploratory purposes it is adequate to consider a simple model (Model IV) wherein the GRB rate is modeled just as a step function with higher rate at large redshifts ($z > 3$) when the average metallicity of the Universe is low, and taken to have a lower rate when the Universe is metal-rich at lower redshifts. This transition in the assumed GRB rate which is assumed to mimic the change in the mean metallicity of the Universe is taken to occur abruptly at $z = 3$. While metals are produced as a consequence of SF, by construction, Model IV bears no relation to a SFR, this was done for simplicity. The predictions for the expected redshift distribution of GRBs under these assumptions for Model IV are also plotted in Fig. 2.

3 OBSERVATIONS OF GRBS

In order to predict the redshift distribution of GRBs, in addition to a phenomenological model for the SF, we need to model the observed properties of the bursts, their number counts and luminosity distribution. The isotropically emitted photon flux P detected within an energy band $E_1 < E < E_2$ arising from a GRB at redshift z with a luminosity distance $d_L(z)$ is given by,

$$P = \frac{(1+z) \int_{E_1}^{E_2} S(E) dE}{4 d_L^2(z)} \text{ erg s}^{-1}; \quad (2)$$

where $S(E)$ is the differential rest-frame photon luminosity of the source. The total burst luminosity in a given band can then be computed by integrating $E S(E)$ over the relevant energy range. Given a normalized LF $\phi(L)$ for GRBs, the burst rate of observed peak fluxes in the interval $(P_1; P_2)$ is

$$\frac{dN}{dt} (P_1 < P < P_2) = \int_0^{z_1} dz \frac{dV(z) R_{\text{GRB}}(z)}{1+z} \int_{L(P_1; z)}^{L(P_2; z)} dL \phi(L^0(P)); \quad (3)$$

where $dV = dz$ is the comoving volume element, $R_{\text{GRB}}(z)$ is the comoving GRB rate density, $\phi(P)$ is the detector efficiency, and the $(1+z)^{-1}$ is the cosmological time dilation factor. The comoving volume element is given by:

$$\frac{dV}{dz} = \frac{c}{H_0 (1+z)^2} \left[\frac{1}{M} (1+z)^3 + \frac{1}{K} (1+z)^2 + \frac{1}{J} \right]; \quad (5)$$

where Ω_s is the solid angle spanned by the survey. We adopted the detector efficiency function for BATSE provided by Band et al. (2003) to find our best-fit parameters for the GRB LF.

GRBs have a broad LF when uncorrected for beaming effects, however the data are insufficient at the present time to directly determine $\langle L \rangle$ from observations. Therefore, we model the number counts as done by several authors (Porciani & Madau 2001; Guetta et al. 2005) by assuming that the burst luminosity distribution does not evolve with redshift. A simple parametric form is chosen for $\langle L \rangle$,

$$\langle L \rangle / \frac{L}{L_0} = \exp \left(-\frac{L}{L_0} \right); \quad (6)$$

where L denotes the peak luminosity in the 30(2000 keV energy range (rest frame), β is the asymptotic slope at the bright end, and L_0 is a characteristic cutoff luminosity. The normalization $\int_0^\infty \langle L \rangle dL = 1$, is used to define the constant of proportionality in eqn.(6). To describe the typical spectrum of a GRB, we use the form proposed by Band et al. (1993):

$$S(E) = A \begin{cases} \frac{E}{100 \text{ keV}} & \text{exp} \left(-\frac{E}{E_b} \right) & E < E_b \\ \frac{E_b}{100 \text{ keV}} & \text{exp} \left(-\frac{E}{E_b} \right) & E > E_b \end{cases}$$

The energy spectral indices, α and β , have the values -1 and -2.25 , respectively, measured from the bright BATSE bursts by Preece et al. (2000), with a spectral break at $E_b = 511 \text{ keV}$. This description has been successfully calibrated against the observed number counts by Porciani & Madau (2001) which we adopt. They in turn used the off-line BATSE sample of Komersar et al. (2000), which includes 1998 archival BATSE ("triggered" plus "non-triggered") bursts in the 50(300 keV band.

We then optimize to determine the value of the 3 free parameters in the LF, β and L_0 and the normalization constant, for the different SF history models considered here. The overall quality of the best-fit in the χ^2 -sense is slightly better for our semi-analytic SF model (Model II) as it is slightly lower at high redshifts ($z > 5$) compared to the Porciani & Madau model. This is due to the fact that increasing star formation at high redshift causes the over-prediction of the number of bursts to be consistent with the faintest off-line BATSE counts. We find that increasing the steepness of the high-luminosity tail of $\langle L \rangle$ requires an increase in L_0 for the same value of β , implying that both models studied here need the presence of relatively high-luminosity events to reproduce the data. On comparing the properties of the LFs that provide the best-fit for each star formation rate, we also find that the typical burst luminosity increases in models with larger amounts of star formation at early epochs as also shown by Lloyd-Ronning et al. (2002). However, two of the star formation models considered here, Model I and Model II, predict a very similar redshift distribution for GRBs. This is due to the fact that although the SF for these models appears to diverge at $z > 7$, there is not much time elapsed at these high redshifts. Therefore, we only show the predicted distribution for Model II in Fig. 2.

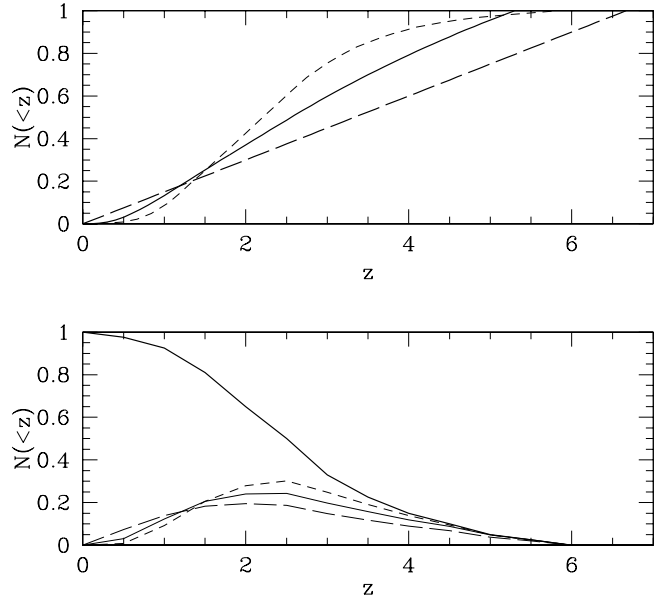


Figure 2. Top panel: The predicted cumulative fraction of GRBs as a function of redshift for various models studied here. The solid curve is the prediction for Model II, the short-dashed curve for Model III and the long-dashed curve is for Model IV. Note that Models III and IV are normalized with respect to Model II. Bottom panel: We illustrate the effect of folding in the detection efficiency of SWIFT as currently modeled by Mortson & Sollerman (2005). Despite the fall-off in sensitivity for $z > 6$ bursts as indicated by the thin solid line curve, the SFR models will still be distinguishable for about 1000 detected bursts. The conventions for the line-type are as before: thick solid [Model II]; long-dashed [Model IV] and short-dashed [Model III].

For our Model III, with significantly lower amounts of star formation, fewer bursts are predicted at higher redshift compared to Models I and II. Folding in the detection efficiency model curve for SWIFT (Mortson & Sollerman 2005), we predict the observed GRB redshift distribution for SWIFT (see Fig. 2).

4 RESULTS AND CONCLUSIONS

Our best-fit parameters for the LF of GRBs, combined with BATSE number counts and the peak-flux distribution for observed bursts are then used to predict the redshift distribution for GRBs given a SFR model. The results for the SFR models and the metallicity dependent rate model are plotted in Fig. 2. The predicted z -distribution for Models I and II are very similar, and we show the curve only for Model II. For both Models I and II, we find that a very large fraction (75%) of all GRBs originate at redshifts of four or lower. Our results are in excellent agreement with those reported recently by Guetta et al. (2005), where they studied the luminosity and angular distribution of long duration GRBs, similarly modeling the SFR history (in particular see their Fig. 3). Note that Guetta et al. utilize the relation between an assumed jet angular distribution and

³ The best-fit $\chi^2/\text{d.o.f}$ for the models ranges from 0.76 (1.05).

the GRB LF to predict the observed redshift distribution of bursts. They predict a local GRB detection rate for both the structured jet model and the universal jet model that is corrected for beaming. In this work we assume that the energy release in GRBs is isotropic. In an earlier calculation Bromm & Loeb (2002) predicted a higher proportion of GRBs at higher redshifts compared to this work. This discrepancy arises due to the fact their treatment did not include a LF for GRBs and did not take into account the spectral energy distribution of GRBs. Unlike supernovae, GRBs are not standard candles, although there has been a recent claim of a tight correlation between the rest-frame peak energy and the rest-frame beaming corrected gamma-ray energy release (Ghirlanda et al. 2004) which may allow them to be used as standard yardsticks for cosmography purposes (Mortsmann & Sollerman 2005). The inclusion of the LF coupled with the Band function are key ingredients that are needed in order to make robust predictions for the redshift distribution, even though there are considerable uncertainties. For Model III with lower SFRs at high redshifts, we find a much smaller fraction of GRBs only about 10% to originate from $z > 4$. It is interesting to note that our toy Model IV predicts (not surprisingly) a higher proportion of bursts 40% at $z > 4$.

Our Model IV assumes that as low-mass galaxies are likely to have statistically lower metallicities, they are likely to contain more luminous GRBs than high-mass galaxies. Given that galaxies assemble hierarchically through mergers, then it is also possible that the highest redshift GRBs could be systematically more luminous owing to the lower mass and metallicity of their hosts. Such an effect motivates the metallicity dependence of the GRB rate assumed here. Additionally, SF activity is likely to be enhanced in merging galaxies. In major mergers of gas-rich spiral galaxies, this enhancement takes place primarily in the inner kiloparsec. Metallicity gradients in the gas are likely to be smoothed out, by both mixing prior to SF and supernova enrichment during the starburst. GRB luminosities could thus be suppressed in such well-mixed galaxies, making GRBs more difficult to detect in these most luminous objects, in which a significant fraction of all high-redshift star formation is likely to have occurred. Shocks in tidal tails associated with merging galaxies are also likely to precipitate the formation of high-mass stars, yet as tidal tails are likely to consist of relatively low-metallicity gas, it is perhaps these less intense sites of star formation at large distances from galactic radii that are more likely to yield detectable GRBs. As more SWIFT bursts are followed-up and their environments are better studied, this correlation will be testable.

Given the current uncertainties and our lack of knowledge of high redshift star formation, if SWIFT detects a handful of bursts from beyond $z \sim 6$ with measured redshifts, these bursts might end up providing the only observational constraint on the SF at these early epochs (see Fig. 2). We find that for a large number, of say, 1000 detected bursts, we will be able to discriminate between the various SFR models as illustrated in Fig. 3. Note that a more accurate and calibrated detection efficiency curve for SWIFT will be available after a few years of operation. The robustness of the assumption that the SFR is a good proxy for the GRB rate can also be tested further in the near future as the uncertainties due to dust correction in determining SFRs are better understood and the host galaxies of GRBs

are studied in more detail. As we explore here, the relation between averaged metallicity of the Universe and GRB rate might also prove to be testable with future observations of GRB host galaxies.

ACKNOWLEDGMENTS

We thank Elena Rossi, Daphne Guetta, Eli Waxman and an anonymous referee for useful suggestions that have improved the paper.

REFERENCES

- Ahn, S. H. 2000, *ApJ*, 520, L9
- Andersen et al., 2000, *A & A*, 364, L54
- Band et al., 1993, *ApJ*, 413, 281
- Becker, B., et al., 2001, *AJ*, 122, 2850
- Berger, E., et al., 2003, *ApJ*, 588, 99
- Blain, A., & Natarajan, P., 2000, *MNRAS*, 312, L35
- Blain, A., et al., 1999, *MNRAS*, 309, 715
- Bromm, V., & Loeb, A., 2002, *ApJ*, 575, 111
- Christensen, L., Hjorth, J., & G0rosabel, J., 2004, *A & A*, 425, 913
- Cole, L., et al., 1994, *MNRAS*, 271, 781
- Courty et al., 2004, *MNRAS*, 354, 581
- Dickinson, M., et al., 2003, *ApJ*, 587, 25
- Fan, X., et al., 2001, *AJ*, 122, 2833
- Fynbo, J., et al., 2003, *A & A*, 406, L63
- Galam, T., et al., 1998, *Nature*, 395, 670
- Gehrels, N., et al., 2004, *ApJ*, 611, 1005
- Gou, L., et al., 2004, *ApJ*, 604, 508
- G0rosabel, J., et al., 2004, *A & A*, 427, 87
- Guetta, D., Piran, T., & Waxman, E., 2005, *ApJ*, 619, 412
- Hjorth, J., et al., 2003, *ApJ*, 697, 699
- Izzard et al., 2004, *MNRAS*, 348, 1215
- Jakobsson, P., et al., 2005, *MNRAS*, in press, astro-ph/0505542
- Kaumann, G., Guiderdoni, B., & White, S., 1993, *MNRAS*, 267, 981
- Kogut, A., et al., 2003, *ApJS*, 148, 161
- Kombers et al., 2000, *ApJ*, 533, 696
- Kulkarni, S. R., Djorgovski, S. G., Ramaprakash, A. N., et al. 1998, *Nature*, 393, 35
- Lamb, D., & Reichart, D., 2000, *ApJ*, 536, 1
- Lloyd-Ronning, N., et al., 2002, *ApJ*, 574, L554
- MacFadyen, A., & Woosley, S., 1999, *ApJ*, 524, 262
- Madau, P., et al., 1996, *MNRAS*, 283, 1388
- Malesani, D., et al., 2004, *ApJ*, 609, L5
- M0ller, P., Fynbo, J. P. U., Hjorth, J., et al. 2002, *A & A*, 396, L21
- Pettini, R., 2003, *The Messenger*, 111, 13
- Preece et al., 2000, *ApJS*, 126, 19
- Porciani, C., & Madau, P., 2001, *ApJ*, 548, 522
- Ramirez-Ruiz, R., et al., 2002, *ApJ*, 565, L9
- Ramirez-Ruiz, R., Trentham, N., & Blain, A., 2002, *MNRAS*, 329, 465
- Shapley, A. E., Steidel, C. C., Pettini, M., et al. 2003, *ApJ*, 588, 65
- Somerville, R., & Livio, M., 2003, *ApJ*, 593, 611
- Spergel, D., et al., 2003, *ApJS*, 148, 175
- Stanek, K., et al. 2003, *ApJ*, 591, L17
- Steidel, C., et al., 2004, *ApJ*, 604, 534
- Tanvir, N., et al., 2004, *MNRAS*, 352, 1073
- Totani, T., 1997, *ApJ*, 486, L71
- Vreeswijk et al., 2004, *A & A*, 419, 927
- Wijers, R., Bloom, J. S., Bagla, J., & Natarajan, P., 1998, *MNRAS*, 294, L13